International Journal for Multidisciplinary Research (IJFMR)
E-ISSN: 2582-2160 ● Website: www.ijfmr.com ● Email: editor@ijfmr.com

Power Quality Improvement in Distribution Systems Using A Robust Hybrid Series Active Power Filter

P. Manjusha[1], P. Sridevi[2], Avv Srinivas[3]

[1,2,3]Associate Professor, Dept. Of Eee, Vsm College Of Engineering, Ramachandrapuram, A.P, India

Abstract:
Current and voltage harmonics are one of the most well-known power quality problems and are solved by using a series hybrid active power filter (HSAPF). Deteriorating power quality has an adverse economic impact on utilities and customers. In this article, a new controller design is proposed that utilizes a sliding-mode controller (S2) to increase the robustness and stability of the HSAPF. An accurate averaging model of a three-phase HSAPF is also derived. The design concept of the robust HSAPF has been verified through simulation and experimental studies, and the results obtained are discussed.

Keywords: Averaging model, series hybrid active power filter, power quality, robust series hybrid active power filter (HSAPF), sliding-mode controller.

I. INTRODUCTION

In recent years, the enormous increase in the use of nonlinear loads has raised numerous power quality issues, such as high current harmonics, voltage distortion, and low power factor in the electrical grid [1]. To meet the need for improved power quality, different topologies of active power filters (series active filters and shunt active filters) are connected to the nonlinear load. These filters are the most widely used solution, as they effectively eliminate the current distortion and reactive power produced by nonlinear loads.

Therefore, the proliferation of nonlinear loads in the system generates harmonic currents that are injected into the AC power lines. This distorted supply voltage and current causes some protection devices to malfunction, transformers and motors to burn out, and cables to overheat. Therefore, it is essential to install compensation devices for the harmonic currents and voltages produced by nonlinear loads. Traditionally, passive power filters (PPFs) have been used as a compensation device to offset the distortion generated by constant nonlinear loads. These filters [2] are designed to provide a low-impedance path for harmonics and maintain good power quality with a simple design and low cost. However, passive filters have some disadvantages, such as mismatch, resonance, dependence on power supply system conditions, and large passive component values leading to bulky implementations.

However, they are generally expensive and have high operating losses [3], [4]. To overcome these disadvantages and improve compensation performance with a lower cost of active power filters (APFs), Peng et al., in 1988 [5], introduced a novel HAPF-III topology, in which the APF is connected in series with the source and nonlinear load, and the PPF is connected in parallel with the load, acting as a power factor correction capacitor. This topology [6] has received much attention for its ability to withstand high load currents and functions as a harmonic isolator between the source and the nonlinear load.

Control strategy is important for improving the performance of a series hybrid active power filter (SAPF). In fact, many articles on hybrid power filters have already proposed advanced techniques to reduce current harmonics generated by these nonlinear loads. In [7], a linear feedback-forward controller for a hybrid power filter is designed. But this controller is not easy to obtain both steady-state and transient-state performances with the linear control strategy because the dynamic model of HSAPF system contains multiplication terms of control inputs and state variables. Due to the nonlinear characteristics of HSAPF, a sliding mode controller is presented in [8]. Sliding mode control is known as an appropriate control technique to control nonlinear systems with uncertain dynamics and disturbances due to its order reduction property and low sensitivity to disturbances and plant parameter variations, which reduces the burden of exact modeling requirement. Moreover, this sliding mode control also decreases the design complexity of feedback control by decoupling the system into individual lower-dimensional subsystems. Due to these given properties, the implementation of sliding mode control can be found in the areas of power electronic switching devices. The principle of sliding mode control is defined to enforce sliding mode motion on the predefined switching surfaces of the system state space using discontinuous control. Switching surfaces must be selected such that the sliding motion maintains the desired dynamics according to a given performance criterion. Conventional control methods, such as the linear-quadratic regulator [9] or the linear-quadratic Gaussian servo controller [10] for linear systems, are required to choose suitable switching surfaces. The discontinuous control must then be chosen such that any state outside the discontinuous surface is forced to reach the surface within a finite time. Consequently, the sliding mode occurs along the surface and the system follows the desired dynamics.

The main difficulty in the hardware implementation of a classical sliding-mode control method is vibrato. This is nothing more than an undesirable oscillation phenomenon with finite frequency and amplitude. This vibrato is dangerous due to the system's control precision, the high wear of moving mechanical parts, and high heat losses in electrical circuits. Vibrato occurs due to unmodeled dynamics. These unmodeled dynamics are created by servomechanisms, sensors, and data processors with smaller time constants. In sliding-mode control, the switching frequency must be considerably high to make the controller more robust, stable, and vibrato-free, as vibrato decreases with increasing system switching frequency. In sliding-mode controller applications in power converter systems, the vibrato problem can naturally be reduced by increasing the switching frequency. However, this is not possible in the case of power converters due to certain limitations in the switching frequency caused by losses in the power converters, resulting in vibrato. Therefore, this vibration problem cannot be blamed on the sliding mode implementation as it is mainly caused by switching limitations. In [11], it is shown that vibration exponentially tends to zero if the relative degree of the system with actuators or sensors is 2. The relative degree of HSAPF system is 2. Due to this relative degree of HSAPF system and also because of these obstacles in a classical sliding mode controller, this paper proposes a new controller i.e. Sliding Mode Controller-2 (SMC-2).

This proposed controller suppresses vibration and improves the performance of HSAPF. This controller is completely new for this HSAPF system topology. A recent research paper [12] focuses on Carrier-based Pulse Width Modulation (CBPWM) for HSAPF topology. But in some cases, CBPWM-based HSAPF may not be fully measurable in most of the real-world situations. In the CBPWM case, power system disturbances have not been considered, and furthermore, the presence of a delay in the reference tracking point results in a slow response of the overall system. Therefore, the tracking error is not effectively reduced, and system stability is minimally improved. To address this, SMC-2 is proposed for a voltage-source converter. The idea behind this controller is to achieve gain stability, perfect tracking, and distortion-free load current and voltage. In view of the aforementioned issues, the development of a robust controller with a faster reference tracking approach in HSAPF, which accommodates all disturbances such as load voltage distortion, parametric load variation, source current distortion, and supply voltage unbalance, is prioritized to improve the compensation capability of the HSAPF system.

This article is organized as follows. Section II describes the system topology schematic and the hardware modules of the three-phase HSAPF model. Section III describes the averaged modeling of the HSAPF system. Section IV describes the controller design for the HSAPF. Section V describes the simulation and experimental results of harmonic compensation using the HSAPF. Section VI presents the conclusions of this article.

I. DESCRIPTION OF THE SYSTEM TOPOLOGY SCHEMATIC AND HARDWARE MODULES OF THE HSAPF MODEL

Figures 1 and 2 show the experimental prototype and the schematic diagram of the HSAPF developed in the laboratory.

Fig. 1. (a) Experimental setup of the SAPF. (b) Experimental setup of the HSAPF.

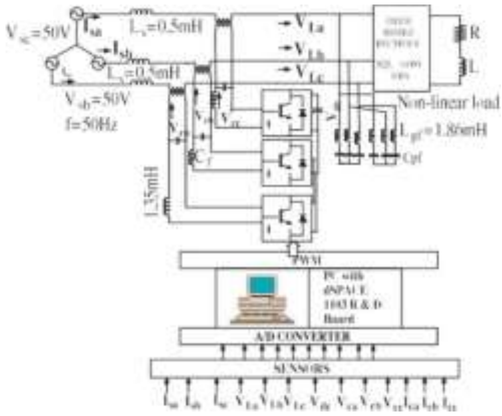

Fig. 2. Schematic diagram of the control and power circuit of the HSAPF.

This HSAPF topology consists of a series-connected active power filter (SAPF) and a shunt-connected PPF. The PPF is connected in parallel with the load. The PPF consists of a fifth and seventh tuned LC filter of varying rating (Lpf = 1.86 mH and Cpf = 60 µF) for compensation of harmonic current on the load side. The SAPF is connected in series with the supply via a 1:2 turns ratio matching transformer to ensure galvanic isolation. The SAPF consists of three parts: a SEMIKRON inverter based on a three-phase IGBT, a 2200 µF DC-link capacitor, and a high-frequency three-phase LC filter with matching impedances (Cf = 60 µF, Lf = 1.35 mH). The high-frequency LC filter is applied to remove high-frequency switching ripples from the compensation voltage supplied by the inverter. A non-linear load consisting of a three-phase diode bridge rectifier (SQL 100 V, 100 A) with a load RL (i.e., an 8.5 A, 100 Ω resistor and a 40 mH coil) is considered. Seven voltage sensors (LEM LV 25-P) and three current sensors (LEM LA 55-P) are required. The sensors detect voltages and currents and send their input to the dSPACE 1103 R&D board.

TABLE I
System parameters used for simulation and experiment
Line voltage and frequency: Vs = 50 V (RMS), f = 50 Hz
Line impedance: Ls = 0.5 mH, Rs = 0.1 Ω
Nonlinear load impedance: L = 40 mH, R = 100 Ω, 8.5 A
Active series filter parameter: Cf = 60 µF, Lf = 1.35 mH, Cdc = 2200 µF, Vdc = 40 V
Passive shunt filter parameter: Lpf = 1.86 mH, Cpf = 60

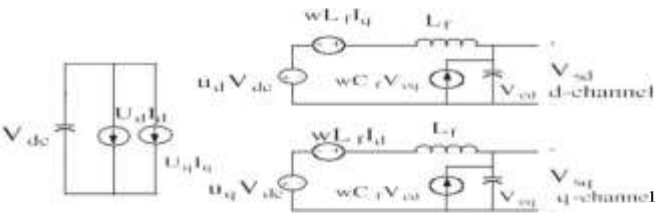

Fig. 3. Averaged equivalent circuit in a three-phase stationary frame of the HSAPF

implemented with dSPACE 1103. First, the controller is implemented using MATLAB/Simulink. The real-time workshop is used to produce C code for real-time applications. The interface between MATLAB/Simulink and dSPACE 1103 allows the control algorithm to be executed. The basic control structure and its mathematical equations are presented in Section IV. The switching signals are generated from the slave DSP. The generated switching pulse is used as input for the amplifier circuit.
The function of an amplifier circuit is to convert 5 to 15 V. The amplifier circuit consists of a CD4504 chip and an HCPL 2601 isolation circuit. The output of the amplifier circuit acts as input
for the inverter controller. For its implementation, the control algorithm is implemented with a fixed step size of 100 µs and, therefore, the maximum switching frequency of a PWM voltage source inverter (VSI) of the HSAPF is fixed at 10

Results and Discussions

Simulation Results

The reference generation approach (HSRF method) with the switching pattern generation scheme (i.e., SMC-2) of the HSAPF system shown in Fig. 2 is tested using MAT-LAB/Simulink software. A three-phase source voltage is applied to a harmonic voltage-generating nonlinear load. This voltage-generating nonlinear load consists of a three-phase controller.

For satisfactory operation of the HSAPF system, this controller satisfies the stability condition.

C. Stability Analysis of the HSAPF Based on a Sliding Mode Controller

This section analyzes the stability of the HSAPF system with the suggested control strategy. For the stability analysis of the external dynamics of the Vdc and Vcq system, we define a sliding collector as follows:

A diode bridge rectifier supplies an RL load. Due to this type of nonlinear load, harmonic distortion occurs in both the source current and the load voltage. This harmonic pollution is the cause of power quality disturbances. Therefore, power quality disturbances can be eliminated using HSAPF. The simulation and experimental parameters are summarized in Table I. A reference generation technique and a modulation technique, i.e., the hybrid control approach-based SRF (HSRF) method and the sliding-mode controller-based HSAPF, are verified and analyzed using the following simulation results in MATLAB. To verify the reliability of the proposed controller, the system is simulated in MATLAB/Simulink version 2010. The simulation objective is to reduce the total harmonic distortion (THD) response of the sliding-mode controller-based HSAPF below 5%. An HSRF combined with the sliding-mode controller technique, whose time derivative is [context needed for "total harmonic thrash"]. The use of DC link voltage for generating equivalent control law is based on proper utilization of source voltage Vs, load current IL, source current Is, steady state DC voltage Vdc and dynamic load condition [context needed for "dynamic load"]. The existing method is presented in Figure 6. The nature of unfiltered source current is exactly same as load current active filters.

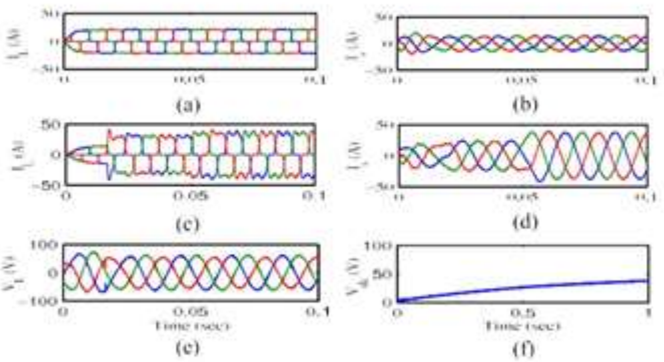

Fig. . 6. (a) Steady-state response of the load current before compensation. (b) Steady-state response of the source current after compensation. (c) Transient response of the load current before compensation. (d) Transient response of the source current after compensation. (e) Load voltage after compensation. (f) DC-link voltage for the existing method (ideal sliding-mode controller).

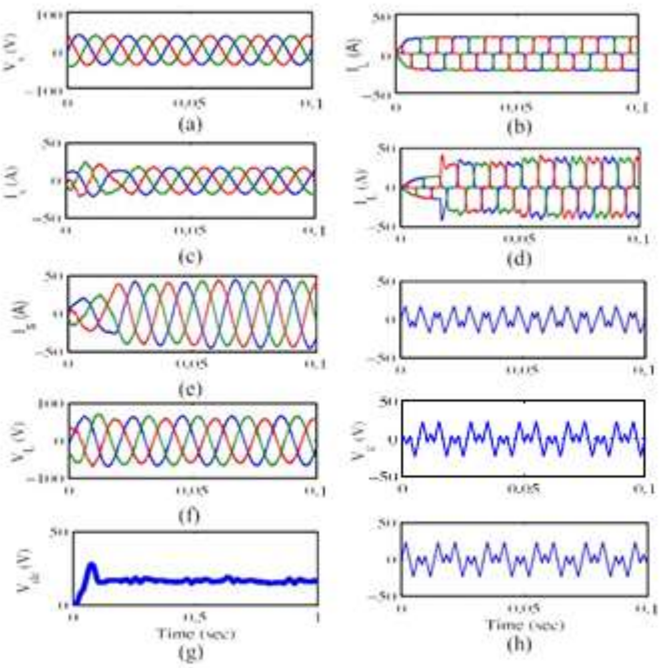

Fig . 7. (a) Source voltage. (b) Steady-state response of the load current before compensation. (c) Steady-state response of the source current after com- pensation. (d) Transient response of the load current before compensation.

(e) Transient response of the source current after compensation. (f) Load voltage after compensation. (g) DC-link voltage. (h) Three-phase compensating voltage for the proposed controller-based HSAPF system.

MATLAB simulation results for source voltage *Vs*, load current *IL* , source current *Is*, dc voltage *Vdc* for steady state, dynamic condition of load, and parametric variation of the HSAPF system under SMC-2 have been depicted in Figs. 7 and 8. From the simulation results, it is proved that the THD response of the sliding-mode-controller-based HSAPF is smaller than the THD response of the existing technique-based HSAPF. Simulation results under several system operating conditions of load have verified the design concept of the suggested highly effective and robust sliding-mode-based HSAPF. The robustness of the proposed HSAPF has been analyzed here. In the proposed

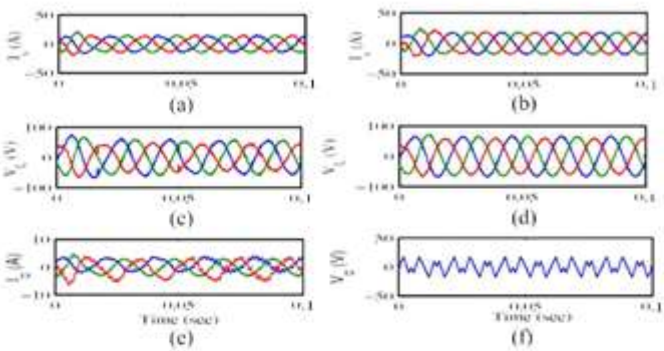

Fig. 8. (a) Three-phase source current after compensation for the existing controller-based HSAPF. (b) Three-phase source current after compensation for the proposed controller-based HSAPF. (c) Three-

phase load voltage after com- pensation for the existing controller-based HSAPF. (d) Three-phase load voltage after compensation for the proposed controller-based HSAPF. (e) Three-phase compensating current. (f) Compensating voltage for phase-a in the parametric variation case of the HSAPF system.
controller, the source current THD is reduced from 20.14% to 1.62%. For the transient condition of load, the THD of source current for the proposed controller-based HSAPF is reduced from 26.7% to 2.16%. The harmonic compensation ratio (HCR) for steady state and the parametric variation of the HSAPF system case are approximately the same, but the HCR in the transient case of the nonlinear load is differed by only 0.55% from the above two cases. Thus, the THDs of the source current are unaffected by the parametric variations of load. This proves the robustness of the proposed HSAPF under parametric variations of load. The HCR factor is calculated as follows:

$$HCR = \frac{\text{THD (\%) After Compensation}}{\text{THD (\%) Before Compensation}} * 100\%$$

A. ***Experimental Results***

The proposed control algorithm has been implemented in real-time on the hardware setup developed in our laboratory. A prototype of the experimental setup is shown in Fig. 1. The effectiveness of the proposed scheme is compared with the existing method [15] (Harmonic Series Compensators in Power Systems: Their Sliding Mode Control), in which instantaneous reactive power theory is used as the reference generation process and an ideal sliding mode controller with carrier-based PWM is applied for the switching pattern generation. The disadvantage of this controller is the switching frequency, i.e., it requires a high switching frequency to make the system more robust and stable, but it produces more switching losses, vibrations, and white Gaussian noise. But in the case of the proposed approach, SMC-2 is employed as the voltage controller, i.e., for the switching pattern generation and HSRF method is employed for the reference voltage generation in the HSAPF. Experimental studies for steady-state and dynamic conditions are performed and discussed in the following sections.
Case 1: Balanced Supply Voltages With Steady-State Load Condition: The performance of the proposed HSAPF is veri- fied through load impedance in the initial case. A diode bridge

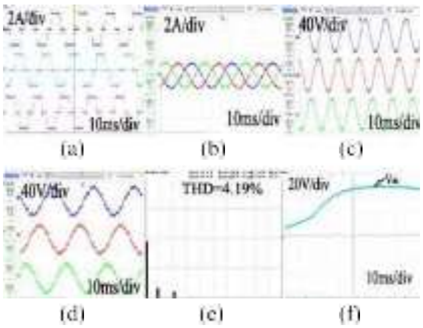

Fig. 9. *Case 1a:* (a) Three-phase load current before compensation.
(b) Three-phase source current after compensation. (c) Three-phase load volt- age before compensation.
(d) Three-phase load voltage after compensation.
(e) THD of the source current after compensation. (f) DC-link voltage in the existing method.

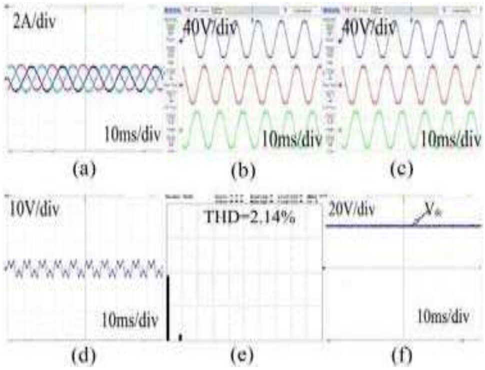

Fig. 10. *Case 1b:* (a) Three-phase source current after compensation.
(b) Three-phase load voltage before compensation. (c) Three-phase load volt- age after compensation. (d) Compensating voltage for phase-a. (e) THD of the source current after compensation. (f) DC-link voltage in the proposed method.

rectifier with an *RL* load is selected as the test load to mea- sure the operation of the HSAPF for load compensation. The three-phase load currents (ILa , ILb , ILc) before compensation are shown in Fig. 9(a). The source current is found to be sinu- soidal. The source current, the load voltage, and the reference tracking behavior of the compensating voltage for both the ex- isting and proposed methods have been presented in Figs. 9 and 10, respectively.

Case 2: Balanced Supply Voltages With Steady-State Load Condition as Well as Changing HSAPF Parameters: In this case, the HSAPF parameters are changed from Cf = 50 μF, Lf = 0.35 mH to Cf = 60 μF, Lf = 1.35 mH. Under this condition, the performance of the proposed controller has been verified with the existing method through Figs. 11 and 12. It is seen that in the case of the proposed approach, the source cur- rent are smooth and distortion is less as compared to the existing method. Hence, the effective harmonic compensation is more in the case of the proposed method. Also, the THD response of the source current after compensation is superior in the case of the proposed method over the existing method.

CASE 3: Balanced Supply Voltages With Dynamic Load Condition: The performance of the proposed HSAPF, assum-

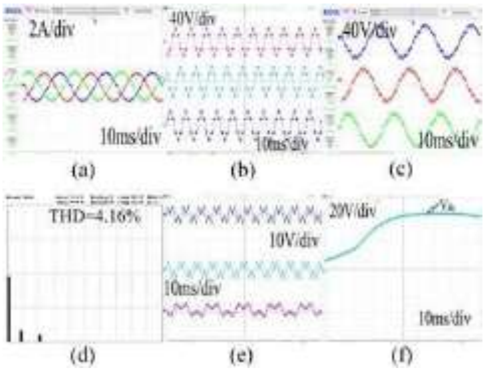

Fig. 11. *Case 2a:* (a) Three-phase source current after compensation. (b) Load voltage before compensation. (c) Load voltage after compensation. (d) THD of the source current after compensation. (e) Three-phase compensating voltage.

(f) DC-link voltage in the exist method (ideal sliding-mode controller).

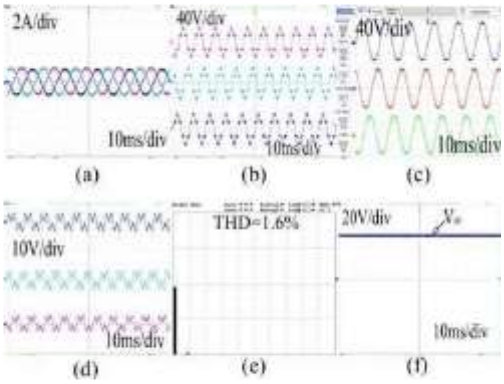

Fig. 12. *Case 2b:* (a) Three-phase source current after compensation. (b) Three-phase load voltage before compensation. (c) Three-phase load volt- age after compensation. (d) Three-phase compensating voltage. (e) THD of the source current after compensation. (f) DC-link voltage for the proposed method.

ing the balanced supply voltages, during a sudden load varying condition is illustrated in Figs. 13 and 14. To create dynamic condition, the load is changed from (R = 100 Ω, L = 40 mH) to (R = 20 Ω, L = 10 mH). When the load changes, the com- pensating voltage quickly responds to changes to compensate the harmonic voltage and current in the load, as shown in Fig. 13. Also, the compensated source current can be viewed from Figs. 13(a) and 14(b) for both existing and proposed meth- ods. As noticed, the HSAPF system with the proposed approach achieves better performances in comparison to existing one. Furthermore, the dc-link voltage in the case of existing method settles to the reference value with a time delay of 0.1 s, while a delay of only 0.024 s is possible for the proposed technique, as illustrated in Figs. 13(d) and 14(c). Figs. 13 and 14 shows that the source current THD is effectively reduced from 25.9% to 2.16% and 3.25% in the proposed and existing methods, respectively. Therefore, this transient event demonstrates the actual capability and enhances the performance of the proposed approach over the existing approach.

Case 4: Unbalanced Supply Voltages With Steady-State Load Condition: In the previous cases, the supply voltage has been considered as sinusoidal and balanced, but this voltage

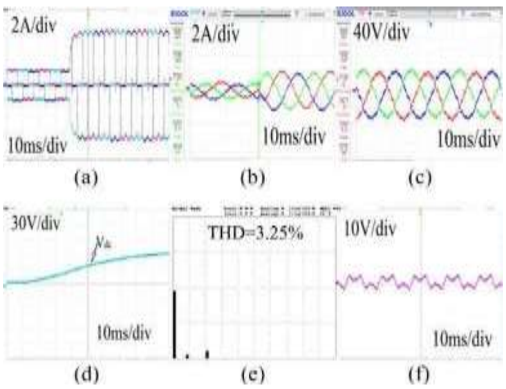

Fig. 13. *Case 3a:* (a) Three-phase load current before compensation.
(b) Three-phase source current after compensation. (c) Three-phase load voltage after compensation. (d) DC-link voltage. (e) THD of the source current after compensation. (f) Compensating voltage for phase-a.

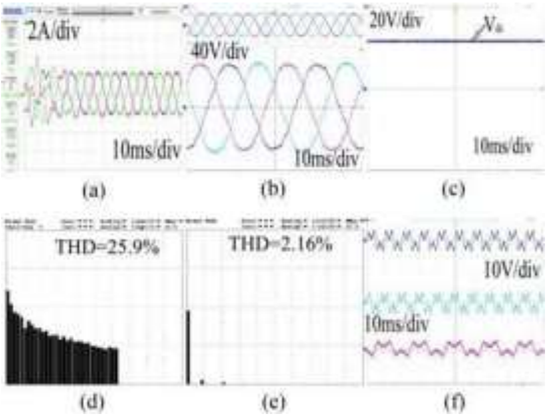

Fig. 14. *Case 3b:* (a) Three-phase source current after compensation.
(b) Three-phase load voltage after compensation. (c) DC-link voltage. (d) THD of the source current before compensation. (e) THD of the source current after compensation. (f) Three-phase compensating voltage after compensation in the proposed method.

is considered as unbalanced in nature. To verify the effective- ness of the proposed control algorithm under such a condition, experiments have been carried out. The profiles for three-phase supply voltages and source currents are shown in Figs. 15 and 16, respectively. Fig. 16 shows that the harmonic compensation per- formance of the HSAPF has not been deteriorated at the unbal- anced source voltage condition and the source currents are also balanced. But, a small number of flickers are observed in the case of the existing method. THD analysis for phase-a supply current is shown in Figs. 15 and 16; the proposed method has lower THD (i.e., 2.16%) as compared to the existing method (i.e., 3.25%), whereas the load current is distorted with a THD factor of 26.7%.

It is verified through experiments that the proposed controller-
based HSAPF has better steady-state performances as well as better dynamic responses as compared to the existing approach. In addition, to evaluate the robustness performance of the exist- ing controller and the proposed controller assuming previously mentioned four cases, HCR factors are calculated and summa- rized in Table II. The results of Table II demonstrate that in

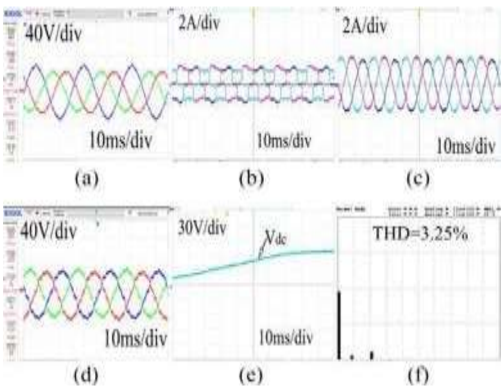

Fig. 15. *Case 4a:* (a) Three-phase source voltage before compensation.
(b) Three-phase load current before compensation. (c) Three-phase source current after compensation. (d) Three-phase load voltage after compensation.
(e) DC-link voltage. (f) THD of the source current after compensation.

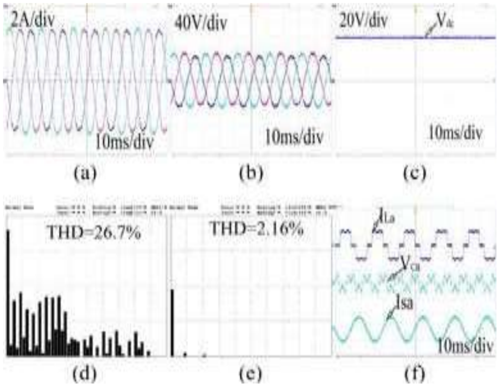

Fig. 16. *Case 4b:* (a) Three-phase source current after compensation.
(b) Three-phase load voltage after compensation. (c) DC-link voltage. (d) THD of the source current before compensation. (e) THD of the source current after compensation. (f) Compensating voltage with the load current and the source current after compensation in the proposed method.

TABLE II
Harmonics Compensation Effect of the Proposed and Existing Control Strategy in the HSAPF (Experimental)
Cases THD % phase-a source current HCR (%)

	Methods used in HSAPF	Before comp. THD (%)	After comp. THD (%)	
Case 1	Proposed method	24.5	2.14	8.73
	Existing method	24.5	4.19	17.1
Case 2	Proposed method	20.14	1.6	7.94
	Existing method	20.14	4.16	20.65
Case 3	Proposed method	25.9	2.16	8.33
	Existing method	25.9	3.25	12.54
Case 4	Proposed method	26.7	2.16	8.08
	Existing method	26.7	3.25	12.17

the case of the proposed approach, HCR factors are maintained nearly the same, i.e., 8%, and these factors are unaffected by any perturbations raised in load or source sides, such robustness cannot be achieved by using the existing control strategy, in which the HCR factor has been largely deviated in the presence the case of the proposed approach, HCR factors are maintained nearly the same, i.e., 8%, and these factors are unaffected by any perturbations raised in load or source sides, such robustness cannot be achieved by using the existing control strategy, in which the HCR factor has been largely deviated in the presence of steady-state and parametric variation behavior of the load. Thus, the superiority of the proposed algorithm over the exist- ing method has been highlighted through all situations of power system perturbations.

Conclusion

In this article, a new robust controller design for HSAPF is presented. The control design is established using SMC-2, which derives the equivalent control law. This control law is very useful for generating switching patterns. The robustness of the proposed controller has been verified by analyzing its performance under steady-state and transient power system conditions. With the application of this technique, the functionalities of the HSAPF are improved. From the obtained simulations, as well as experimental results, it has been observed that the proposed HSAPF provides efficient mitigation of current and voltage harmonics, reference voltage tracking behavior, and reactive power compensation under dynamically varying load conditions. In the presence of additive white noise, switching losses, and distortion in both the source current and load voltage, the SRF method proves to be the most suitable for generating reference patterns. Furthermore, the key feature of SMC-2 is its variable-structure control method, which reduces tracking error distortion, suppresses vibration and noise, and achieves perfect gain stability for the HSAPF system. The proposed filter can compensate for source currents and also automatically adjust to offset variations in nonlinear load currents, maintain steady-state DC-link voltage, and assist in correcting the power factor of the adjacent power supply. Simulation and experimental results under various system operating load conditions have verified that the suggested sliding-mode HSAPF design concept is highly effective and robust..

References

1. Z. Zeng, H. Yang, S. Tang, and R. Zhao, "Objective-oriented power quality compensation of multifunctional grid-tied inverters and its application in microgrids," *IEEE Trans. Power Electron.*, vol. 30, no. 3, pp. 1255–1265, Mar. 2015.
2. A. B. Nassif, W. Xu, and W. Freitas, "An investigation on the selection of filter topologies for passive filter applications," *IEEE Trans. Power Del.*, vol. 24, no. 3, pp. 1710–1718, Jul. 2009.
3. M. Ali, E. Laboure, and F. Costa, "Integrated active filter for differential- mode noise suppression," *IEEE Trans. Power Electron.*, vol. 29, no. 3, pp. 1053–1057, Mar. 2014.
4. E. R. Ribeiro and I. Barbi, "Harmonic voltage reduction using a series active filter under different load conditions," *IEEE Trans. Power Electron.*, vol. 21, no. 5, pp. 1394–1402, Sep. 2006.
5. F. Z. Peng, H. Akagi, and A. Nabae, "A new approach to harmonic com- pensation in power systems-a combined system of shunt passive and se- ries active filters," *IEEE Trans. Ind. Appl.*, vol. 26, no. 6, pp. 983–990, Nov./Dec. 1990.
6. S. Diptimayee Swain, P. K. Ray, and K. Mohanty, "Voltage compensation and stability analysis of hybrid series active filter for harmonic compo- nents," in *Proc. Annu. IEEE India Conf.*, 2013, pp. 1–6.
7. W. Tangtheerajaroonwong, T. Hatada, K. Wada, and H. Akagi, "Design and performance of a transformerless shunt hybrid filter integrated into a three-phase diode rectifier," *IEEE Trans. Power Electron.*, vol. 22, no. 5, pp. 1882–1889, Sep. 2007.

8. W. Guo, J. Wu, and D. Xu, "A novel sliding mode control of a high-voltage transformerless hybrid shunt active power filter," in *Proc. 4th IEEE Conf. Ind. Electron. Appl.*, 2009, pp. 2908–2913.
9. B. Kedjar and K. Al-Haddad, "DSP-based implementation of an LQR with integral action for a three-phase three-wire shunt active power filter," *IEEE Trans. Ind. Electron.*, vol. 56, no. 8, pp. 2821–2828, Aug. 2009.
10. R. Panigrahi, B. Subudhi, and P. C. Panda, "A robust LQG servo control strategy of shunt-active power filter for power quality enhancement," *IEEE Trans. Power Electron.*, vol. 31, no. 4, pp. 2860–2869, Apr. 2016.
11. L. M. Fridman, "Singularly perturbed analysis of chattering in relay con- trol systems," *IEEE Trans. Autom. Control*, vol. 47, no. 12, pp. 2079–2084, Dec. 2002.
12. M. A. Mulla, R. Chudamani, and A. Chowdhury, "A novel control method for series hybrid active power filter working under unbalanced supply conditions," *Int. J. Elect. Power Energy Syst.*, vol. 64, pp. 328–339, 2015.
13. S. Rahmani, K. Al-Haddad, and H. Y. Kanaan, "Average modeling and hybrid control of a three-phase series hybrid power filter," in *Proc. IEEE Int. Symp. Ind. Electron.*, 2006, vol. 2, pp. 919–924.
14. S. D. Swain and P. K. Ray, "Harmonic current and voltage compensation using HSAPF based on hybrid control approach for synchronous reference frame method," *Int. J. Elect. Power Energy Syst.*, vol. 75, pp. 83–90, 2016.
15. H. De Battista and R. J. Mantz, "Harmonic series compensators in power systems: Their control via sliding mode," *IEEE Trans. Control Syst. Tech- nol.*, vol. 8, no. 6, pp. 939–947, Nov. 2000.